

This article was downloaded by:

On: 22 January 2011

Access details: *Access Details: Free Access*

Publisher *Taylor & Francis*

Informa Ltd Registered in England and Wales Registered Number: 1072954 Registered office: Mortimer House, 37-41 Mortimer Street, London W1T 3JH, UK



## Journal of Coordination Chemistry

Publication details, including instructions for authors and subscription information:

<http://www.informaworld.com/smpp/title~content=t713455674>

### Synthesis, crystallographic, and theoretical investigation of *fac*-[Re<sup>I</sup>(salen)(CO)<sub>3</sub>(S)] complexes, salen = monocharged bidentate Schiff-base and S = pyridine, CH<sub>3</sub>OH

Alice Brink<sup>a</sup>; Hendrik G. Visser<sup>a</sup>; Andreas Roodt<sup>a</sup>

<sup>a</sup> Department of Chemistry, University of the Free State, Bloemfontein 9300, South Africa

First published on: 07 December 2010

**To cite this Article** Brink, Alice, Visser, Hendrik G. and Roodt, Andreas (2011) 'Synthesis, crystallographic, and theoretical investigation of *fac*-[Re<sup>I</sup>(salen)(CO)<sub>3</sub>(S)] complexes, salen = monocharged bidentate Schiff-base and S = pyridine, CH<sub>3</sub>OH', *Journal of Coordination Chemistry*, 64: 1, 122 – 133, First published on: 07 December 2010 (iFirst)

**To link to this Article:** DOI: 10.1080/00958972.2010.538050

**URL:** <http://dx.doi.org/10.1080/00958972.2010.538050>

PLEASE SCROLL DOWN FOR ARTICLE

Full terms and conditions of use: <http://www.informaworld.com/terms-and-conditions-of-access.pdf>

This article may be used for research, teaching and private study purposes. Any substantial or systematic reproduction, re-distribution, re-selling, loan or sub-licensing, systematic supply or distribution in any form to anyone is expressly forbidden.

The publisher does not give any warranty express or implied or make any representation that the contents will be complete or accurate or up to date. The accuracy of any instructions, formulae and drug doses should be independently verified with primary sources. The publisher shall not be liable for any loss, actions, claims, proceedings, demand or costs or damages whatsoever or howsoever caused arising directly or indirectly in connection with or arising out of the use of this material.

# Synthesis, crystallographic, and theoretical investigation of *fac*-[Re<sup>I</sup>(salen)(CO)<sub>3</sub>(S)] complexes, salen = monocharged bidentate Schiff-base and S = pyridine, CH<sub>3</sub>OH

ALICE BRINK, HENDRIK G. VISSER\* and ANDREAS ROODT\*

Department of Chemistry, University of the Free State,  
PO Box 339, Bloemfontein 9300, South Africa

(Received 14 August 2010; in final form 1 October 2010)

Two rhenium(I) complexes of the form *fac*-[Re(L-L')(CO)<sub>3</sub>(S)] were synthesized (L-L' = N-O salen-type bidentate ligand, S = coordinating methanol or pyridine) and the crystal structures of *fac*-[tricarbonylmethanol-(2-(3-methylbutyliminomethyl)phenolato)rhenium(I)] and *fac*-[tricarbonyl-(2-(3-methylbutyliminomethyl)phenolato)pyridinerhenium(I)] are reported. The influence of the coordinating neutral monodentate ligand in these *fac*-[tricarbonyl(N,O-salen)rhenium(I)] complexes was investigated both in solid state and at theoretical level using X-ray diffraction, IR, NMR, and DFT calculations.

**Keywords:** Rhenium; Salen; N-O bidentate ligand; Crystal structure

## 1. Introduction

Interest in rhenium and technetium complexes bearing the *fac*-M(CO)<sub>3</sub><sup>+</sup> entity (M = Tc(I), Re(I)) as potential diagnostic and therapeutic radiotracers in the treatment of cancer has increased tremendously [1–4] due to the fact that the *fac*-[M(CO)<sub>3</sub>]<sup>+</sup> core is inert while the water molecules bound to it are quite labile [5]. It therefore comes as no surprise that several promising compounds have been synthesised over the past few years using these tri-carbonyl synthons [6–10].

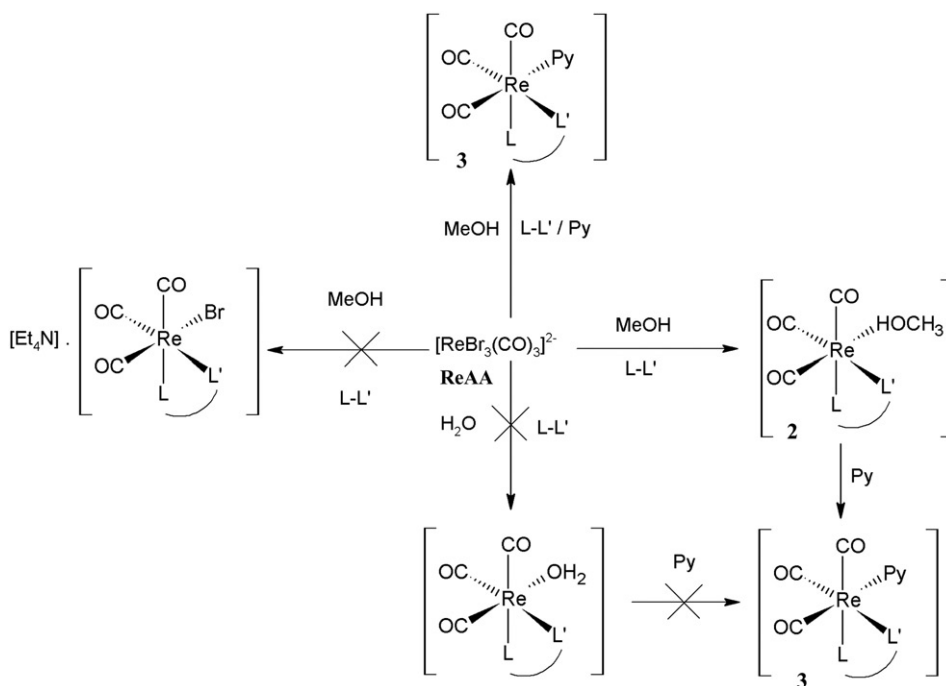
One approach to the design of potential radiopharmaceuticals is the so-called mixed ligand [2 + 1] approach proposed by Mundwiler *et al.* [11]. This approach offers a variety of options to the designer, since the bidentate ligand could be used as a chelator with a directing ligand attached to it, while the third labile position on the rhenium metal center is occupied by another ligand, which simply acts as a “blocker” to nucleophilic attack from other biomolecules *in vivo*. Another option is that the third position is occupied by a directing ligand while the bidentate ligand simply offers stability in terms of chelation.

Fundamental chemical knowledge of the *fac*-tricarbonylrhenium(I) complexes will afford more effective design of complexes to be used as radiopharmaceuticals.

\*Corresponding authors. Email: visserhg@ufs.ac.za; roodta@ufs.ac.za

This knowledge includes stability evaluations, formation kinetics, and the development of new synthetic pathways. A few limitations must however be considered when designing experimental procedures for radiopharmaceuticals for routine clinical application. The restrictions require the synthetic procedures to occur in one step, a high purity yield, ideal biomolecule concentration, and the experimental time dependent on the half-life of the radionuclide. An important limitation which must also be kept in mind is that any preparation is performed in saline solution (0.9% NaCl in water or buffer) [5]. Therefore, the majority of fac-M(CO)<sub>3</sub><sup>+</sup> complexes synthesized to date has focused on water as solvent, although the study of these complexes in various solvents have led to interesting spectroscopic and photochemical results [12–14].

Our interest is to investigate the possible use of Schiff-base ligands in the [2 + 1] approach, since coordination chemistry of Schiff-bases has received much interest due to their ability to form stable complexes with most transition metals [15]. These compounds display potential as ligands and are generally prepared by condensation of primary amines with a carbonyl precursor [16]. The versatility of Schiff-bases, in particular salicylaldiminates, allows for mono- and bi-valent bidentate ligands with varying electronic and steric effects afforded by the substituent on the nitrogen atom [17, 18]. Moreover, the introduction of a biological active amine onto a relatively small backbone holds great promise. However, all our efforts to synthesize fac-[Re(CO)<sub>3</sub>(salen)X]<sup>n-</sup> complexes (X = H<sub>2</sub>O, Br<sup>-</sup>, py) from aqueous medium proved to be extremely difficult since these reactions almost always formed oily products and gave low yields. This led us to use methanol as an alternative solvent (scheme 1). As a result,



Scheme 1. General reaction scheme of [Re(L-L')(CO)<sub>3</sub>(S)] synthesis (L-L' = mono-anionic bidentate ligand, Py = pyridine, S = coordinating ligand).

we propose here a new synthetic route for the synthesis of mixed ligand complexes of rhenium tricarbonyls. The crystal structures of *fac*-[tricarbonylmethanol-(2-(3-methylbutyliminomethyl)phenolato)rhenium(I)] **2**, and *fac*-[tricarbonyl-(2-(3-methylbutyliminomethyl)phenolato)pyridinerhenium(I)] **3**, are included as part of this study. This is the first published crystal structure of a complex of *fac*-[Re(CO)<sub>3</sub>(L-L')(CH<sub>3</sub>OH)]<sup>n-</sup>.

## 2. Experimental

### 2.1. Materials and general procedures

All reagents used for synthesis and characterization were of analytical grade, purchased from Sigma-Aldrich, unless otherwise stated. Reagents were used as received, without purification. Rhenium pentacarbonyl bromide was purchased from Strem Chemicals, Newburyport, US. *fac*-[NEt<sub>4</sub>]<sub>2</sub>[ReBr<sub>3</sub>(CO)<sub>3</sub>] (**ReAA**) was synthesized as described by Alberto *et al.* [19]. <sup>13</sup>C- and <sup>1</sup>H FT-NMR spectra of the rhenium compounds were recorded at 150.96 and 600.28 MHz, respectively, on a Bruker AXS 600 MHz at 25°C in CD<sub>3</sub>OD (3.31 ppm) and C<sub>3</sub>H<sub>6</sub>O (2.05 ppm); chemical shifts are reported in ppm. Infrared spectra were recorded on a Bruker Tensor 27 Standard System spectrophotometer with a laser range of 4000–370 cm<sup>-1</sup>, equipped with a temperature cell regulator, accurate within 0.3°C. Solid samples were analyzed as KBr pellets and liquid samples in methanol solution in an NaCl liquid cell. All data were recorded at room temperature. UV-Vis spectra were collected on a Varian Cary 50 Conc UV-Visible Spectrophotometer, equipped with a Julabo F12-mV temperature cell regulator (accurate within 0.1°C) in a 1.000 ± 0.001 cm quartz cuvette cell. Computational calculation results were obtained using the GAUSSIAN-03W [20] software package. DFT calculations were done at the B3LYP [21] level of theory with the 6–31G++(d,p) [22, 23] basis set for the main group elements and LanL2Dz for rhenium, using the High Performance Computing Facility of the University of the Free State. Optimized structures were verified as minima through frequency analysis. Graphical representations of overlays of selected complexes are obtained with Hyperchem 7.52 [24].

### 2.2. Synthesis of salen-3MeBu (1)

The ligand 2-(3-methylbutyliminomethyl)phenol (salen-3MeBu) was synthesized according to the method previously reported [25]. Salicylaldehyde (1.40 g, 11.5 mmol) was dissolved in 30 mL methanol, to which 3 g of anhydrous MgSO<sub>4</sub> was added, and 3-methylbutylamine (14.0 mmol, 1.00 g, 11.5 mmol) dissolved in methanol (10 mL) was then added dropwise to this mixture. The reaction was heated to 80° and refluxed for 3 h. MgSO<sub>4</sub> was filtered off and solvent removed under reduced pressure to yield the yellow oil product (Yield: 1.61 g, 73.5%). <sup>1</sup>H-NMR (600 MHz, acetone-d<sub>6</sub>) δ 8.53 (s, 1H, HC=N), 7.37 (m, 1H, Ar), 7.31 (m, 1H, Ar), 6.87 (m, 2H, Ar), 3.65 (dt, 2H, *J* = 7.2, 1.3 Hz), 1.72 (m, 1H), 1.58 (q, 2H, *J* = 7.2 Hz), 0.96 (d, 6H, *J* = 6.5 Hz). <sup>13</sup>C-NMR (600 MHz, acetone-d<sub>6</sub>) δ 165.43 (C1), 161.25, 131.90, 131.41, 119.10, 118.32, 116.50 (Ar), 57.28, 39.82, 25.69, 21.86 (C24, C25).

### 2.3. Synthesis of [Re(salen-3MeBu)(CO)<sub>3</sub>(HOCH<sub>3</sub>)] (2)

Salen-3MeBu (0.0169 g,  $8.84 \times 10^{-5}$  mol) dissolved in methanol (5 mL) was added to ReAA (0.0623 g,  $8.09 \times 10^{-5}$  mol) in methanol (5 mL). The reaction was stirred for 24 h at room temperature. A yellow, micro-crystalline product was obtained upon evaporation of the solvent. Yellow crystals suitable for X-ray diffraction were obtained by slow evaporation of solvent (Yield: 0.024 g, 38%). IR (KBr,  $\text{cm}^{-1}$ ):  $\nu_{(\text{CO})}$  2001.4 (vs), 1876.5 (vs). UV-Vis (nm;  $\text{L mol}^{-1} \text{cm}^{-1}$ ):  $\lambda_{\text{max}} = 382.9$ ,  $\epsilon = 1.311 \times 10^3$ . <sup>1</sup>H-NMR (600 MHz, acetone-d<sub>6</sub>)  $\delta$  8.22 (s, 1H, HC=N), 7.15 (m, 2H, Ar), 6.65 (d, 1H, Ar,  $J = 8.5$  Hz), 6.42 (m, 1H, Ar), 1.68 (m, 5H), 0.99 (d, 3H,  $J = 6.5$  Hz), 0.93 (d, 3H,  $J = 6.5$  Hz). <sup>13</sup>C-NMR (600 MHz, acetone-d<sub>6</sub>)  $\delta$  166.78 (C1), 166.24, 136.23, 134.54, 122.77, 121.53, 113.92 (Ar), 69.14, 41.99, 26.54, 23.12, 22.64.

### 2.4. Synthesis of [Re(salen-3MeBu)(CO)<sub>3</sub>(NC<sub>5</sub>H<sub>5</sub>)] (3)

Salen-3MeBu (0.027 g,  $1.43 \times 10^{-4}$  mol) dissolved in methanol (5 mL) was added to a methanol (10 mL) solution of ReAA (0.1 g,  $1.30 \times 10^{-4}$  mol). The reaction was stirred for 6 h at 25°C before addition of pyridine (0.015 g,  $1.95 \times 10^{-4}$  mol), in 5 mL methanol, followed by a further 12 h stirring. The pale yellow precipitate was filtered and dried. Crystals suitable for X-ray diffraction were obtained from slow evaporation of the filtrate (Yield: 0.0152 g, 22%). The addition of pyridine to a methanol solution of **2**, after stirring for 4–6 h and allowing solvent evaporation, also yielded **3**. IR (KBr,  $\text{cm}^{-1}$ ):  $\nu_{(\text{CO})}$  2013.6 (vs), 1904.8 (w), and 1878.4 (vs). UV-Vis (nm;  $\text{L mol}^{-1} \text{cm}^{-1}$ ):  $\lambda_{\text{max}} = 389.0$ ,  $\epsilon = 2.038 \times 10^3$ . <sup>1</sup>H-NMR (600 MHz, acetone-d<sub>6</sub>)  $\delta$  8.69 (m, 2H, Ar), 8.33 (s, 1H, HC=N), 8.03 (tt, 1H, Ar,  $J = 7.8, 3.2, 1.6$  Hz), 7.55 (m, 2H, Ar), 7.27 (m, 1H, Ar), 7.14 (dd, 1H, Ar,  $J = 7.8, 1.8$  Hz), 6.79 (d, 1H, Ar,  $J = 8.5$  Hz), 6.50 (m, 1H, Ar), 4.23–4.04 (m, 2H), 1.62 (m, 1H), 1.80–1.57 (m, 2H), 0.94 (d, 3H,  $J = 6.5$  Hz), 0.91 (d, 3H,  $J = 6.5$  Hz). <sup>13</sup>C-NMR (600 MHz, acetone-d<sub>6</sub>)  $\delta$  166.75 (C1), 165.41, 152.05, 139.28, 135.46, 134.64, 125.92, 122.09, 120.58, 114.53 (Ar), 68.08, 40.83, 25.71, 22.03, 21.61.

### 2.5. Structure analysis and refinement

Diffraction data for **2** were collected on a Bruker ApexII 4K CCD diffractometer using Mo-K $\alpha$  (0.71073 Å) and  $\omega$ -scans at 100(2) K. All reflections were merged and integrated with SAINT-PLUS [26] and corrected for Lorentz, polarization, and absorption effects using SADABS [27]. The data for **3** were collected on an Oxford Diffraction Xcalibur 3 CrysAlis CCD system [28] using Mo-K $\alpha$  (0.71073 Å) and  $\omega$ -scans at 100(2) K. Intensity data were extracted and integrated using CrysAlis RED [29]. Both structures were solved by the heavy atom method and refined through full-matrix least-squares cycles using SHELX-97 [30] as part of the WinGX [31] package with  $\Sigma(|F_o| - |F_c|)^2$  being minimized. All non-H atoms were refined with anisotropic displacement parameters, while hydrogens were constrained to parent atom sites using a riding model [aromatic C–H = 0.95 Å { $U_{\text{iso}}(\text{H}) = 1.2 U_{\text{eq}}$ }; aliphatic C–H = 0.98 Å { $U_{\text{iso}}(\text{H}) = 1.5 U_{\text{eq}}$ }]. The graphics were obtained with the Visual Crystal Structure Information System software DIAMOND [32]; crystallographic details are summarized in table 1. Selected bond lengths and angles of **2** and **3** are listed in tables 2 and 3. Distances and angles involving selected hydrogen-bonding interactions of **2** are given in table 4. Figures 1–3 represent

Table 1. General X-ray crystallographic data and refinement parameters for [Re(salen-3-MeBu)(CO)<sub>3</sub>(S)] (S = coordinating ligand).

Compound	<b>2</b>	<b>3</b>
Empirical formula	ReNO <sub>5</sub> C <sub>16</sub> H <sub>20</sub>	ReN <sub>2</sub> O <sub>4</sub> C <sub>20</sub> H <sub>21</sub>
Formula weight	492.53	539.60
Temperature (K)	100(2)	100(2)
Wavelength (Å)	0.71069	0.71073
Crystal system	Monoclinic	Monoclinic
Space group	<i>C2/c</i>	<i>P2<sub>1</sub>/c</i>
Unit cell dimensions (Å, °)		
<i>a</i>	19.3075(8)	12.9051(4)
<i>b</i>	13.8078(6)	8.6642(3)
<i>c</i>	13.7882(6)	18.6961(5)
$\alpha$	90.0	90.0
$\beta$	110.299(2)	105.279(3)
$\gamma$	90.0	90.0
Volume (Å <sup>3</sup> ), <i>Z</i>	3447.6(3), 8	2016.57(11), 4
Calculated density (g cm <sup>-3</sup> )	1.898	1.777
Absorption coefficient (mm <sup>-1</sup> )	7.072	6.052
<i>F</i> (000)	1904	1048
Crystal color	Yellow	Yellow
Crystal morphology	Cuboid	Cuboid
Crystal size (mm <sup>3</sup> )	0.34 × 0.10 × 0.08	0.36 × 0.20 × 0.15
$\theta$ range for data collection (°)	1.85–27.99	2.26–28.00
Completeness	100.0%	99.7%
Index ranges	<i>h</i> = –25 to 23 <i>k</i> = –18 to 16 <i>l</i> = –18 to 17	<i>h</i> = –17 to 15 <i>k</i> = –11 to 11 <i>l</i> = –14 to 24
Reflections collected	20559	15447
Independent reflections	4179 [ <i>R</i> (int) = 0.0412]	4867 [ <i>R</i> (int) = 0.0226]
Refinement method	Full-matrix least-squares on <i>F</i> <sup>2</sup>	Full-matrix least-squares on <i>F</i> <sup>2</sup>
Data/restraints/parameters	4179/3/221	4867/0/244
Goodness-of-fit on <i>F</i> <sup>2</sup>	1.047	0.983
Final <i>R</i> indices [ <i>I</i> > 2 $\sigma$ ( <i>I</i> )]	<i>R</i> <sub>1</sub> = 0.0379, <i>wR</i> <sub>2</sub> = 0.0699	<i>R</i> <sub>1</sub> = 0.0208, <i>wR</i> <sub>2</sub> = 0.0455
<i>R</i> indices (all data)	<i>R</i> <sub>1</sub> = 0.0496, <i>wR</i> <sub>2</sub> = 0.0741	<i>R</i> <sub>1</sub> = 0.0331, <i>wR</i> <sub>2</sub> = 0.0500
$\rho_{\max}$ and $\rho_{\min}$ (e Å <sup>-3</sup> )	1.889 and –2.784	0.787 and –0.761

Table 2. Selected interatomic bond lengths (Å) and angles (°) for **2**.

Re(1)–O(1)	2.117(4)	O(03)–C(03)	1.139(8)
Re(1)–N(1A)	2.148(7)	O(04)–C(04)	1.406(9)
Re(1)–N(1B)	2.219(16)	C(1)–N(1A)	1.346(11)
Re(1)–C(01)	1.900(6)	C(1)–N(1B)	1.212(18)
Re(1)–C(02)	1.902(6)	O(1)–C(12)	1.331(7)
Re(1)–C(03)	1.891(8)	C(1)–C(11)	1.447(9)
Re(1)–O(04)	2.179(4)	C(11)–C(12)	1.402(8)
O(01)–C(01)	1.152(7)	N(1A)–C(21A)	1.469(10)
O(02)–C(02)	1.165(7)	N(1B)–C(21B)	1.540(30)
O(1)–Re(1)–N(1A)	84.0(2)	C(12)–O(1)–Re(1)	127.4(3)
O(1)–Re(1)–N(1B)	83.5(4)	C(01)–Re(1)–N(1A)	172.0(3)
C(01)–Re(1)–C(02)	86.4(3)	C(01)–Re(1)–N(1B)	170.3(4)
C(03)–Re(1)–C(01)	87.6(3)	C(04)–O(04)–Re(1)	124.5(4)
C(03)–Re(1)–C(02)	88.3(3)	N(1A)–Re(1)–O(04)	76.4(2)
C(03)–Re(1)–O(1)	95.5(2)	C(03)–Re(1)–O(04)	175.1(2)
C(01)–Re(1)–O(1)	93.4(2)	O(1)–Re(1)–O(04)	80.78(14)
C(02)–Re(1)–O(1)	176.2(2)		
O(1)–C(12)–C(1)–N(1A)	3.4(6)	O(1)–C(12)–C(1)–N(1B)	32.1(9)

Table 3. Selected interatomic bond lengths (Å) and angles (°) for **3**.

Re(1)–O(1)	2.1075(19)	O(01)–C(01)	1.152(3)
Re(1)–N(1)	2.172(2)	O(02)–C(02)	1.156(3)
Re(1)–N(2)	2.213(3)	O(03)–C(03)	1.146(4)
Re(1)–C(01)	1.919(3)	N(2)–C(31)	1.340(4)
Re(1)–C(02)	1.901(3)	C(11)–C(1)	1.433(4)
Re(1)–C(03)	1.917(4)	O(1)–C(12)	1.305(3)
N(1)–C(1)	1.290(4)	C(11)–C(12)	1.416(4)
N(1)–C(21)	1.482(4)	C(21)–C(22)	1.517(4)
O(1)–Re(1)–N(1)	86.35(8)	N(1)–C(1)–C(11)	128.8(3)
O(1)–Re(1)–N(2)	81.42(9)	C(1)–N(1)–Re(1)	124.9(2)
N(1)–Re(1)–N(2)	84.27(9)	C(02)–Re(1)–O(1)	175.50(12)
C(02)–Re(1)–C(03)	90.51(13)	C(03)–Re(1)–O(1)	93.90(10)
C(02)–Re(1)–C(01)	88.07(13)	C(01)–Re(1)–O(1)	91.07(10)
C(03)–Re(1)–C(01)	90.04(13)	C(21)–N(1)–Re(1)	119.32(17)
O(1)–C(12)–C(1)–N(1)	3.01(2)	C(1)–N(1)–C(21)–C(22)	102.3(3)

Table 4. Hydrogen bonds for **2** (Å and °).

D–H...A	d(D–H)	d(H...A)	d(D...A)	∠(DHA)
O(04)–H(04)...O(1)#1	0.84	1.85	2.578(5)	143.4
C(1)–H(1)...O(03)#2	0.95	2.51	3.125(11)	122.4
C(13)–H(13)...O(01)#3	0.95	2.48	3.317(8)	146.8

Symmetry transformations used to generate equivalent atoms: #1:  $-x+1, y, -z+3/2$ ; #2:  $x+1/2, -y+3/2, -z+1$ ; #3:  $-x+1, -y+1, -z+1$ .

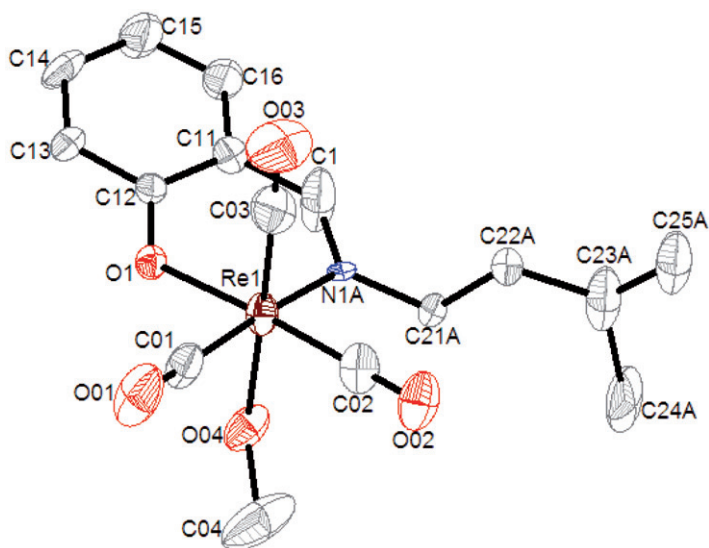


Figure 1. Molecular diagram of **2** showing atom numbering scheme and displacement ellipsoids (50% probability). H-atoms omitted for clarity.



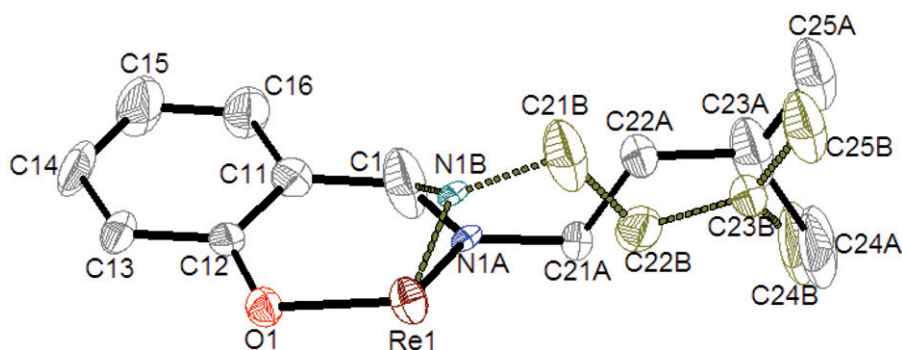


Figure 2. Molecular diagram showing the disorder on the 3-MeBu tail of **2**.

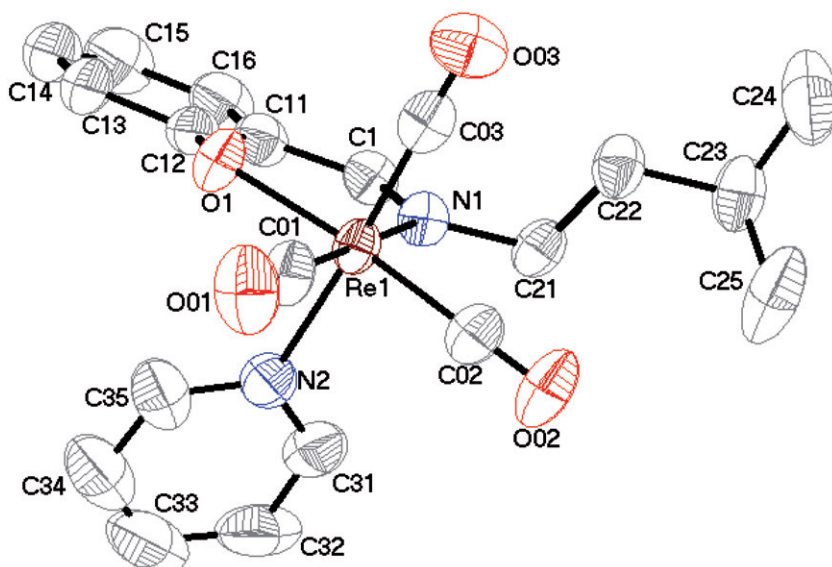


Figure 3. Molecular diagram of **3** showing atom numbering scheme and displacement ellipsoids (50% probability). H-atoms omitted for clarity.

the atom numbering schemes for **2** and **3**, with ellipsoids drawn at 50% probability and hydrogens omitted for clarity.

### 3. Results and discussion

[Re(salen-3MeBu)(CO)<sub>3</sub>(HOCH<sub>3</sub>)] (**2**) and [Re(salen-3MeBu)(CO)<sub>3</sub>(NC<sub>5</sub>H<sub>5</sub>)] (**3**) were synthesized from methanol and single crystals of good enough quality for X-ray data diffraction analysis were obtained. The decision to use methanol as solvent in the synthesis of Re(I)-tricarbonyl complexes with salen ligands proved to be successful for several reasons. First, it was possible to obtain crystallographically pure materials



from methanol as opposed to the impure oils obtained from water. All our attempts to recrystallize these complexes from the water were unsuccessful and addition of a range of organic solvents in an attempt to induce crystallization of these products yielded poor results. In terms of the [2 + 1] approach, we illustrate here that methanol is easily substituted to yield a pure product in satisfactory yield. This certainly creates yet another exciting prospect for the development of a radiopharmaceutical kit using the [2 + 1] approach with these ligand systems. The low yields obtained for **2** and **3** are based on recrystallized products. Yields before recrystallization exceed 80%.

IR spectra of **2** and **3** show strong symmetric and asymmetric bands due to  $\nu_{\text{CO}}$  at 2001.4, 1876.5 and 2013.6, 1904.8, 1878.4  $\text{cm}^{-1}$ , respectively, compared to the ReAA carbonyl bands at 1999.4 and 1867.1  $\text{cm}^{-1}$ . The increase in  $\nu_{\text{CO}}$  stretching frequency from **2** to **3** indicates lower electron density present on Re(I) for **3** [33–36].

All <sup>1</sup>H-NMR spectra exhibit a strong peak at approximately 8 ppm for the imine proton. The effect of increasing electron density is seen in the stepwise upfield shift for **1** ( $\delta$ 8.53), **3** ( $\delta$ 8.33), and **2** ( $\delta$ 8.22). The aromatic protons for **1** and **2** appear at 7.37–6.87 ppm and 7.15–6.42 ppm, respectively. The aromatic protons for **3** including those of pyridine appear at 8.69–6.50 ppm. The methine, methylene, and methyl protons for **1**, **2**, and **3** appear at 3.65–0.96, 1.68–0.93, and 4.23–0.91 ppm. <sup>1</sup>H-NMR spectra for **2** and **3** both indicate rotamers for the 3-MeBu tail. <sup>13</sup>C-NMR data are consistent with <sup>1</sup>H-NMR data. The imine carbon (C1) peak appears at 165.43, 166.78, and 166.75 ppm for **1**, **2**, and **3**. The aromatic carbons appear at 161.25 to 116.50 ppm (**1**), 166.24–113.92 ppm (**2**), and 165.41–114.53 ppm (**3**). Carbons assigned to the 3-MeBu tail appear at 57.28–21.86 ppm (**1**), 69.14–22.64 ppm (**2**), and 68.08–21.61 ppm (**3**).

The crystal structure determinations of **2** (figure 1) and **3** (figure 3) show interesting results. The 3-methyl-butyl substituent is severely disordered over two positions (67–33%) in **2** (figure 2). There are no disorders observed for **3**. All bond distances and angles fall within the expected range for both these complexes. A few classical hydrogen-bonding interactions are observed for **2** (table 4). Both structures are stabilized by weak inter- and intra-molecular hydrogen-bonding interactions.

The octahedron around rhenium(I) is more severely disordered for **2** than for **3**. In **2**, the bidentate salen bite angle at rhenium is 84.0(2)° (O1–Re–N1A) results in large deviations from octahedral geometry, best illustrated by the C03–Re–N1A angle of 100(2)°, and the N1A–Re–O04 angle of 76.4(2)°. To our knowledge, this is the first published crystal structure of a fac-Re(CO)<sub>3</sub><sup>+</sup> complex with a methanol in one of the positions *trans* to a carbonyl. Zobi *et al.* [37] reported a fac-Tc(CO)<sub>3</sub><sup>+</sup> complex containing a coordinated methanol with a Tc–OH–CH<sub>3</sub> bond angle of 128.7(3)° and a Tc–OH bond distance of 2.177(3) Å. The bond distance of the rhenium to O04 (table 2), the methanol oxygen, was calculated as 2.182(4) Å, slightly longer than that found for Re–OH<sub>2</sub> bonds [38, 39] where bond distances to the water oxygen range between 2.153(3) Å and 2.170(5) Å.

Bond distances of the bidentate N and O ligand to rhenium are 2.148(7) and 2.117(4) Å, respectively, and compare well with other N,O ligand-to-metal bond distances which are in the range 2.162–2.186 Å for Re–N and 2.099–2.184 Å for Re–O [11, 38, 40]. The bite angle formed by the salen ligand, and rhenium(I) in **3** is 86.35(8)°, more than two degrees larger than that found for **2**. As a result, less distortion of the octahedron around rhenium in **3** is observed (table 3). Here, the C01–Re–N1 bond angle is only 92.80(10)°. The angle formed by the nitrogen of coordinated pyridine,

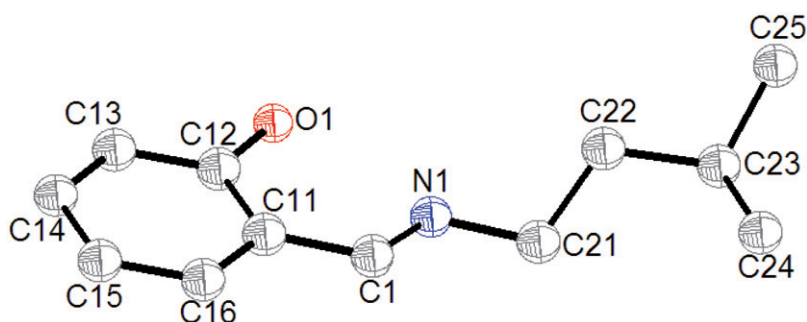


Figure 4. DFT optimized structure of **1**. H-atoms omitted for clarity.

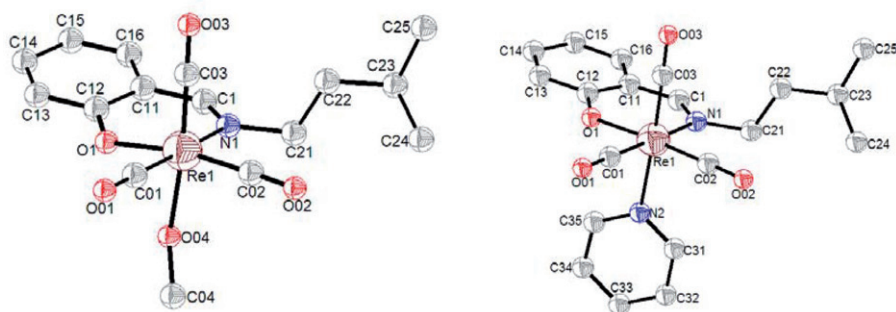


Figure 5. DFT optimized structures of (a) **2** and (b) **3**. H-atoms omitted for clarity.

rhenium, and nitrogen of the bidentate ligand is  $84.27(9)^\circ$ , also closer to ideal octahedral geometry than what was observed for the similar angle formed between the bidentate ligand, rhenium, and methanol in **2**. The Re–N2 bond distance is  $2.213(3) \text{ \AA}$  and compares well with similar complexes [40, 41] where bond distances between  $2.203$  and  $2.230 \text{ \AA}$  were observed. The bonds formed between the N and O donors of the bidentate ligand in **3** of  $2.172(2)$  and  $2.1075(19) \text{ \AA}$ , respectively, are very similar to similar bonds in **2**. These observations, together with the fact that no classical hydrogen-bonding interactions were observed for **3**, lead us to believe that the more severe distortion of the octahedron in **2** is due to hydrogen bonding. This assumption is further supported by the fact that the methanol is involved in a strong hydrogen bond with O1' of the Re' molecule ( $-x+1, y, -z+3/2$ ;  $D-A = 2.578(5) \text{ \AA}$ ).

Calculations are increasingly being used to understand the behavior of metal ions in coordination and organometallic chemistry [42–44]. To compare the factors which determine the crystal structures in the solid state, theoretical structures for **1–3** (figures 4 and 5a,b) were optimized and verified to be a global minimum through frequency calculations. Overlay diagrams of the theoretical molecules with their experimental solid state counterparts are shown in figure 6(a) and (b). The structure of **1** (figure 4) was calculated even though the crystal structure could not be obtained, in order to observe any geometrical trends within these three compounds. The solid state structure of **2** shows good correlation with the DFT optimized structure (figure 6a), with an RMS overlay value of only  $0.21 \text{ \AA}$  (excluding the disordered part of the 3-MeBu group).

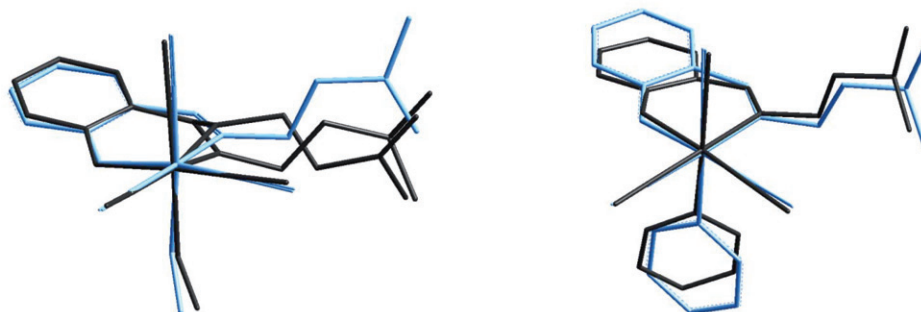


Figure 6. (a) Overlay of the DFT optimized and crystal structures of **2** (RMS value = 0.21 Å). (b) Overlay of the DFT optimized and crystal structures of **3** (RMS value = 1.61 Å). Overlay fits exclude the 3-MeBu group and all hydrogens. The blue structures denote the DFT optimized complexes, while the black structures indicate the solid state structures.

Table 5. Comparison of selected *ligand* geometrical parameters of the crystal structures of **1–3** with their DFT optimized counterparts (Å, °).

	<b>1</b> <sub>DFT</sub>	<b>2</b> <sub>Crystal</sub> <sup>a</sup>	<b>2</b> <sub>DFT</sub>	<b>3</b> <sub>Crystal</sub>	<b>3</b> <sub>DFT</sub>
N(1)–C(1)	1.281	1.346(11)	1.316	1.290(4)	1.318
N(1)–C(21)	1.455	1.469(10)	1.499	1.482(4)	1.498
N(1)–O(1)	2.6321	2.854(10)	2.874	2.929(3)	2.918
C(1)–C(11)	1.456	1.447(9)	1.448	1.433(4)	1.444
O(1)–C(12)	1.341	1.331(7)	1.347	1.305(3)	1.335
C(11)–C(1)–N(1)	122.8	128.0(7)	128.9	128.8(3)	129.4
O(1)–C(12)–C(11)	121.8	122.7(5)	122.2	125.2(3)	123.3
C(1)–N(1)–C(21)	119.5	115.7(7)	115.4	115.8(2)	115.1
N(1)–C(21)–C(22)	110.9	112.2(7)	112.2	112.2(2)	112.4
O(1)–C(12)–C(1)–N(1)	0.11	3.4(6)	8.2	3.1(2)	4.5

<sup>a</sup>Indicates bond distances and angles to the principal fraction of disorder of **2**.

Table 6. Comparison of selected *coordination polyhedral* geometrical parameters of the crystal structures of **2** and **3** with their DFT optimized counterparts (Å, °).

	<b>2</b> <sub>Crystal</sub> <sup>a</sup>	<b>2</b> <sub>DFT</sub>	<b>3</b> <sub>Crystal</sub>	<b>3</b> <sub>DFT</sub>
Re(1)–O(1)	2.117(4)	2.118	2.108(2)	2.120
Re(1)–N(1)	2.148(7)	2.185	2.172(2)	2.188
Re(1)–C(01)	1.900(6)	1.930	1.919(3)	1.932
Re(1)–C(02)	1.902(6)	1.907	1.901(3)	1.905
Re(1)–C(03)	1.891(8)	1.901	1.917(4)	1.922
Re(1)–O(04)/N(2)	2.179(4)	2.243	2.213(3)	2.245
C(03)–O(03)	1.139(8)	1.189	1.146(4)	1.187
C(01)–O(01)	1.152(7)	1.188	1.152(3)	1.186
O(04)–C(04)	1.406(9)	1.470	–	–
O(1)–Re(1)–N(1)	84.0(2)	83.8	86.35(8)	85.3
Re(1)–O(04)–C(04)	124.5(4)	127.4	–	–
N(1)–Re(1)–O(04)/N(2)	76.4(2)	83.9	84.27(9)	86.1
C(01)–Re(1)–C(02)	86.4(3)	89.9	88.07(13)	89.9
Re(1)–N(1)–C(1)	122.2(5)	125.6	124.9(2)	125.5
O(1)–C(12)–C(1)–N(1)	3.4(6)	8.2	3.1(2)	4.5

<sup>a</sup>Indicates bond distances and angles to the principal fraction of disorder of **2**.

The DFT optimized structure of **3**, on the other hand, has a much poorer correlation with its crystallographic counterpart (RMS = 1.61 Å; figure 6b). The pyridine ring rotation and the salen backbone of the crystal structure show significant deviation from the DFT optimized structure. Angles and distances are compared in tables 5 and 6, and quite good agreement exists. Even though the conformations in the crystal and DFT optimized structures are similar, some deviations between the corresponding DFT/solid state structures are clear. These differences between the crystallographic data and the corresponding DFT optimized structures illustrate the net impact of packing effects and intermolecular bonds on the geometrical parameters of the solid state structures.

#### 4. Conclusions

Rhenium salen tricarbonyl complexes were synthesized and crystals suitable for X-ray diffraction were obtained. The coordination of methanol to the rhenium metal center was established as the first example of a rhenium complex of this type reported and discussed. The spectroscopic data indicated the effects of various neutral monodentate ligands have on the rhenium metal center. A theoretical study on the compounds was presented and compared with the corresponding solid state structures.

#### Supplementary material

Crystallographic data for the structures are available free of charge from the Cambridge Crystallographic Data Centre via [www.ccdc.cam.ac.uk](http://www.ccdc.cam.ac.uk) or Email: [data\\_request@ccdc.cam.ac.uk](mailto:data_request@ccdc.cam.ac.uk) as CCDC 801586 and 801587.

#### Acknowledgments

Financial assistance from the University of the Free State is gratefully acknowledged. We thank Prof. Ola Wendt from the University of Lund, Sweden for the use of their Oxford X-ray diffractometer. We also express our gratitude toward SASOL, the South African National Research Foundation (SA-NRF/THRIP), PETLabs Pharmaceuticals, the University of the Free State Strategic Academic Initiative (Advanced Biomolecular Cluster), and the Swedish International Development Cooperation Agency (SIDA) for the financial support for this project. Part of this material is based on the work supported by the SA-NRF/THRIP under grant number GUN 2068915. Opinions, findings, conclusions, or recommendations expressed in this material are those of the authors and do not necessarily reflect the views of the SA-NRF.

#### References

- [1] R. Alberto, R. Schibli, A.P. Schubiger, U. Abram, T.A. Kaden. *Polyhedron*, **15**, 1079 (1996).
- [2] U. Abram, S. Abram, R. Alberto, R. Schibli. *Inorg. Chim. Acta*, **248**, 193 (1996).
- [3] R. Alberto, W.A. Herrmann, P. Kiprof, F. Baumgärtner. *Inorg. Chem.*, **31**, 895 (1992).
- [4] H.H.K. Castro, C.E. Hissink, H.J.H. Teuben, W. Vaalburg, K. Panek. *Recl. Trav. Chim. Pays-Bas*, **111**, 105 (1992).

- [5] R. Alberto, R. Schibli, R. Waibel, U. Abram, A.P. Schubiger. *Coord. Chem. Rev.*, **192**, 901 (1999).
- [6] A. Egli, R. Alberto, R. Schibli, A.O. Schaffland, U. Abram, S. Abram, T.A. Kaden, P.A. Schubiger. *J. Labelled Compounds Radiopharm.*, **37**, 443 (1997).
- [7] R. Alberto, R. Schibli, U. Abram, A. Egli, F.F. Knapp, P.A. Schubiger. *Radiochim. Acta*, **79**, 99 (1997).
- [8] R. Schibli, R. Alberto, U. Abram, S. Abram, A. Egli, P.A. Schubiger, T.A. Kaden. *Inorg. Chem.*, **37**, 3509 (1998).
- [9] R. Alberto, A. Egli, R. Schibli, U. Abram, T.A. Kaden, A.O. Schaffland, R. Schwarzbath, P.A. Schubiger. *Q. J. Nucl. Med.*, **42**, 9 (1998).
- [10] R. Alberto, R. Schibli, A. Egli, P.A. Schubiger, W.A. Herrmann, G. Artus, U. Abram, T.A. Kaden. *J. Organomet. Chem.*, **493**, 119 (1995).
- [11] S. Mundwiler, M. Kündig, K. Ortner, R. Alberto. *Dalton Trans.*, 1320 (2004).
- [12] R. Alberto, A. Egli, U. Abram, K. Hegetschweiler, V. Gramlich, P.A. Schubiger. *J. Chem. Soc., Dalton Trans.*, 2815 (1994).
- [13] D.H. Gibson, B.A. Sleadd, X. Yin. *Organometallics*, **17**, 2689 (1998).
- [14] R. Czerwieniec, A. Kapturkiewicz, R. Anulewicz-Ostrowska, J. Nowacki. *J. Chem. Soc., Dalton Trans.*, 2756 (2001).
- [15] G.J.J. Steyn, A. Roodt, I.A. Poletaeva, Y.S. Varshavsky. *J. Organomet. Chem.*, **536/7**, 197 (1997).
- [16] R. Hernández-Molina, A. Merderos. In *Comprehensive Coordination Chemistry II*, J.A. McCleverty, T.J. Meyer (Eds.), Vol. 1, pp. 411–446, Elsevier, Oxford (2003).
- [17] T. Sasamori, T. Matsumoto, N. Takeda, N. Tokitoh. *Organometallics*, **26**, 3621 (2007).
- [18] É. Tozzo, S. Romero, M.P. dos Santos, M. Muraro, R.H. de A. Santos, L.M. Lião, L. Vizotto, E.R. Dockal. *J. Mol. Struct.*, **876**, 110 (2008).
- [19] R. Alberto, R. Schibli, P.A. Schubiger. *Polyhedron*, **15**, 1079 (1996).
- [20] M.J. Frisch, G.W. Trucks, H.B. Schlegel, G.E. Scuseria, M.A. Robb, J.R. Cheeseman, J.A. Montgomery Jr, T. Vreven, K.N. Kudin, J.C. Burant, J.M. Millam, S.S. Iyengar, J. Tomasi, V. Barone, B. Mennucci, M. Cossi, G. Scalmani, N. Rega, G.A. Petersson, H. Nakatsuji, M. Hada, M. Ehara, K. Toyota, R. Fukuda, J. Hasegawa, M. Ishida, T. Nakajima, Y. Honda, O. Kitao, H. Nakai, M. Klene, X. Li, J.E. Knox, H.P. Hratchian, J.B. Cross, V. Bakken, C. Adamo, J. Jaramillo, R. Gomperts, R.E. Stratmann, O. Yazyev, A.J. Austin, R. Cammi, C. Pomelli, J.W. Ochterski, P.Y. Ayala, K. Morokuma, G.A. Voth, P. Salvador, J.J. Dannenberg, V.G. Zakrzewski, S. Dapprich, A.D. Daniels, M.C. Strain, O. Farkas, D.K. Malick, A.D. Rabuck, F. Raghavachari, J.B. Foresman, J.V. Ortiz, Q. Cui, A.G. Baboul, S. Clifford, J. Cioslowski, B.B. Stefanov, G. Liu, A. Liashenko, P. Piskorz, I. Komaromi, R.L. Martin, D.J. Fox, T. Keith, M.A. Al-Laham, C.Y. Peng, A. Nanayakkara, M. Challacombe, P.M.W. Gill, B. Johnson, W. Chen, M.W. Wong, C. Gonzalez, J.A. Pople. *GAUSSIAN-03*, Revision C.01, Gaussian, Inc., Wallingford, CT (2004).
- [21] A.D. Becke. *J. Chem. Phys.*, **98**, 5648 (2003).
- [22] P.C. Hariharan, J.A. Pople. *Theor. Chim. Acta*, **28**, 213 (1973).
- [23] M.M. Francl, W.J. Pietro, W.J. Hehre, J.S. Binkley, M.S. Gordon, D.J. DeFree, J.A. Pople. *J. Chem. Phys.*, **77**, 3654 (1982).
- [24] Hyperchem<sup>TM</sup> Release 7.52, Windows Molecular Modeling System, Hypercube, Inc. (2002).
- [25] A. Brink, A. Roodt, H.G. Visser. *Acta Cryst.*, **E65**, o3175 (2009).
- [26] Bruker SAINT-PLUS (including XPREP). *Version 7.12*, Bruker AXS Inc., Madison, WI (2004).
- [27] Bruker SADABS. *Version 2004/1*. Bruker AXS Inc., Madison, WI (1998).
- [28] CrysAlis CCD. Oxford Diffraction Ltd., Abingdon, Oxfordshire, UK (2005).
- [29] CrysAlis RED. Oxford Diffraction Ltd., Abingdon, Oxfordshire, UK (2005).
- [30] G.M. Sheldrick. *Acta Cryst.*, **A64**, 112 (2008).
- [31] L.J. Farrugia. *J. Appl. Cryst.*, **32**, 837 (1999).
- [32] K. Brandenburg, H. Putz. *DIAMOND. Release 3.0e*. Crystal Impact GbR, Postfach 1251, D-53002, Bonn, Germany (2004).
- [33] G.J.J. Steyn, A. Roodt, J.G. Leipoldt. *Inorg. Chem.*, **31**, 3477 (1992).
- [34] S. Otto, A. Roodt. *Inorg. Chim. Acta*, **357**, 1 (2004).
- [35] A. Roodt, S. Otto, G. Steyl. *Coord. Chem. Rev.*, **245**, 125 (2003).
- [36] A. Brink, H.G. Visser, A. Roodt, G. Steyl. *Dalton Trans.*, 1246 (2010).
- [37] F. Zobi, B. Spingler, T. Fox, R. Alberto. *Inorg. Chem.*, **42**, 2818 (2003).
- [38] M. Schutte, H.G. Visser. *Acta Cryst.*, **E64**, m1226 (2008).
- [39] M. Schutte, H.G. Visser, A. Roodt. *Acta Cryst.*, **E64**, m1610 (2008).
- [40] R. Czerwieniec, A. Kapturkiewicz, R. Anulewicz-Ostrowska, J. Nowacki. *J. Chem. Soc., Dalton Trans.*, 2756 (2001).
- [41] R. Czerwieniec, A. Kapturkiewicz, R. Anulewicz-Ostrowska, J. Nowacki. *J. Chem. Soc., Dalton Trans.*, 3434 (2002).
- [42] R.D. Adams, B. Captain, C.B. Hollandsworth, M. Johansson, J.L. Smith Jr. *Organometallics*, **25**, 3848 (2006).
- [43] K.P. Gable, A. AbuBaker, K. Zientara, A.M. Wainwright. *Organometallics*, **18**, 173 (1999).
- [44] D.V. Partyka, N. Deligonul, M.P. Washington, T.G. Gray. *Organometallics*, **28**, 5837 (2009).